

# Journal of Visualized Experiments

## Injections of AAV vectors for optogenetics in anesthetized and awake behaving non-human primate brain --Manuscript Draft--

Article Type:	Methods Article - JoVE Produced Video
Manuscript Number:	JoVE62546R2
Full Title:	Injections of AAV vectors for optogenetics in anesthetized and awake behaving non-human primate brain
Corresponding Author:	Yoshiko Kojima, Ph.D. University of Washington Seattle, WA UNITED STATES
Corresponding Author's Institution:	University of Washington
Corresponding Author E-Mail:	ykojima@uw.edu
Order of Authors:	Yoshiko Kojima, Ph.D. Jonathan Ting Robijanto Soetedjo Shane Gibson Gregory Horwitz
Additional Information:	
Question	Response
Please indicate whether this article will be Standard Access or Open Access.	Open Access (US\$4,200)
Please specify the section of the submitted manuscript.	Neuroscience
Please indicate the <b>city, state/province, and country</b> where this article will be filmed. Please do not use abbreviations.	Seattle, WA, USA
Please confirm that you have read and agree to the terms and conditions of the author license agreement that applies below:	I agree to the <a href="#">Author License Agreement</a>
Please provide any comments to the journal here.	
Please indicate whether this article will be Standard Access or Open Access.	Open Access (\$3900)

**TITLE:**

Injections of AAV Vectors for Optogenetics in Anesthetized and Awake Behaving Non-Human Primate Brain

**AUTHORS AND AFFILIATIONS:**

Yoshiko Kojima<sup>1,2</sup>, Jonathan T. Ting<sup>2,3,4</sup>, Robijanto Soetedjo<sup>2,4</sup>, Shane D. Gibson<sup>2</sup>, Gregory D. Horwitz<sup>2,4</sup>

<sup>1</sup>Dept. of Otolaryngology – Head and Neck Surgery, University of Washington, Seattle WA USA.

<sup>2</sup>Washington National Primate Research Center, University of Washington, Seattle WA USA.

<sup>3</sup>Allen Institute for Brain Science, Seattle WA USA.

<sup>4</sup>Dept. of Physiology & Biophysics, University of Washington, Seattle WA USA.

**Email addresses of co-authors:**

Yoshiko Kojima	(ykojima@uw.edu)
Jonathan T. Ting	(JonathanT@alleninstitute.org)
Robijanto Soetedjo	(robi@uw.edu)
Shane D. Gibson	(sgibso@uw.edu)
Gregory D. Horwitz	(ghorwitz@uw.edu)

**Corresponding authors:**

Yoshiko Kojima (ykojima@uw.edu)

**KEYWORDS:**

channelrhodopsin-2, AAV, cerebellum, neocortex, surgery, cannula, enhancers

**SUMMARY:**

As currently implemented, optogenetics in non-human primates requires injection of viral vectors into the brain. An optimal injection method should be reliable and, for many applications, capable of targeting individual sites of arbitrary depth that are readily and unambiguously identified in postmortem histology. An injection method with these properties is presented.

**ABSTRACT:**

Optogenetic techniques have revolutionized neuroscience research and are poised to do the same for gene therapy for neurological disorders. The clinical use of optogenetics, however, requires that safety and efficacy be demonstrated in animal models, ideally non-human primates (NHPs), because of their neurological similarity to humans. The number of candidate vectors that are potentially useful for neuroscience and medicine is vast, and no high throughput means to test these vectors yet exists. Thus, there is a need for techniques to make multiple spatially and volumetrically accurate injections of viral vectors into NHP brain that can be identified unambiguously through postmortem histology. Described herein is such a method. Injection cannulas are constructed from polytetrafluoroethylene (PTFE) tubing coupled to beveled, stainless-steel tubes. These cannulas are autoclavable, disposable, and have low minimal loading volumes, making them ideal for the injection of expensive, highly concentrated viral vector

solutions. An inert, red-dyed mineral oil fills the dead space and forms a visible meniscus with the vector solution, allowing instantaneous and accurate measurement of injection rates and volumes. The oil is loaded into the rear of the cannula, reducing the risk of co-injection with the vector. Cannulas can be loaded in 10 min and injections can be made in 20 min. This procedure is well suited for injection in awake, behaving, or anesthetized animals. When used to deliver high-quality viral vectors, this procedure can produce robust expression of optogenetic proteins, allowing optical control of neural activity and behavior in NHPs.

## INTRODUCTION:

Optogenetics in non-human primates (NHPs) typically involves the injection of viral vectors directly into the brain. One class of vectors that is well suited for this application are those based on adeno-associated virus (AAV). These vectors consist of a protein capsid surrounding a single-stranded DNA genome that, in turn, consists of a promoter, an opsin gene, and optionally other protein-coding and gene-regulatory elements. Advances in molecular cloning and cell culture techniques have facilitated the manipulation and combination of these components for the development of new vectors. Consequently, the collection of AAV vectors that is potentially useful for NHP optogenetics is large and growing rapidly.

At present, the utility of an AAV vector for NHP optogenetics requires testing *in vivo*. This fact is a substantial barrier to progress. Animals must be used sparingly and testing multiple vectors in a single animal requires that injection sites be positioned judiciously relative to neural architecture and well separated relative to viral spread. Accurate histological assessment requires the injections to be spatially and volumetrically accurate. An injection technique previously used for focal delivery of pharmacological agents<sup>1–4</sup> was adapted and simplified to make such injections. This injection technique is inexpensive, uses disposable, sterilizable components, can be used in anesthetized or awake behaving monkeys, and can be used to target diverse brain areas of any depth. The following protocol describes step-by-step procedures for fabricating the disposable components and making the surgical injections in the NHP brain. The advantages and disadvantages of the technique are discussed.

## PROTOCOL:

All experiments were performed in accordance with the Guide for the Care and Use of Laboratory Animals and exceeded the minimal requirements recommended by the Institute of Laboratory Animal Resources and the Association for Assessment and Accreditation of Laboratory Animal Care International. All the procedures were evaluated and approved by the Animal Care and Use Committee of the University of Washington (UW IACUC protocol #4167-01). Five healthy macaques (2 *Macaca mulatta*, 3 *Macaca nemestrina*; male. 4–11 years old) participated in this study. Sterile instruments and technique were used throughout all surgical procedures.

### 1. Making a cannula (Figure 1A)

#### 1.1. Preparation of each part

1.1.1. Blunt the hypodermic needle (30 G, 13 mm length) tip with a disk grinder.

1.1.2. Cut the stainless-steel tubing (30 G, inside diameter = 0.16 mm, outside diameter = 0.31 mm) to a length tailored to the depth of the target brain area (25 mm is well suited to inject the dorsal surface of the cerebral cortex). With a disk grinder, bevel one end of the cut tube and smooth the other. Deburr the inside of the tube with a broach.

1.1.3. Cut the PTFE tubing (inside diameter = 0.23 mm  $\pm$  0.02 mm, wall = 0.23 mm  $\pm$  0.02 mm, 1 mm corresponds to 42 nL  $\pm$  7 nL of fluid) to a length appropriate for the amount of vector solution to be loaded (1  $\mu$ L of vector solution occupies 24 mm of tubing). Flare both ends of the PTFE tube by insertion of the blunted hypodermic needle.

1.2. Insert the blunted hypodermic needle approximately 5 mm into one end of the PTFE tube. Insert the unbeveled end of the stainless-steel tubing approximately 5 mm into the other end (**Figure 1A**).

1.3. Perform pre-injection testing. Inject filtered water through the hypodermic needle hub of the cannula. Confirm that water exits the beveled stainless-steel tubing tip smoothly and that water does not leak from either junction.

## 2. Injection procedure for anesthetized animals

### 2.1. Surgery preparation

2.1.1. Sterilize surgical instruments and supplies using the procedures in the **Table of Materials**.

2.1.2. If needed, take a head MRI for targeting deep brain structures (**Figure 2A**).

2.1.3. Immediately before the surgery, sedate the animals with ketamine (10–15 mg/kg) and administer antibiotics (cefazolin) and analgesics (sustained-release buprenorphine and meloxicam) intramuscularly. Then, deliver propofol via intravenous (IV) catheter in the saphenous or cephalic veins.

2.1.4. Intubate and transit the animal onto isoflurane gas. Confirm proper anesthetization by stable heart rate, blood pressure, respiratory rate, relaxed skeletal muscles, and the absence of palpebral or withdrawal reflexes.

2.1.5. Apply artificial tear ointment to the corneas to prevent drying.

### 2.2. Injection area preparation

2.2.1. Incise the skin and reflect the muscle. Place the manipulator on the stereotaxic frame, position it to aim at the target brain area, and mark the craniotomy position on the skull with a sterilized pen.

2.2.2. Remove the stereotaxic manipulator and perform the craniotomy. Incise the dura if desired (e.g., to visualize sulcal landmarks). Return the manipulator to the stereotaxic frame.

### 2.3. Vector solution loading (Figure 1C)

2.3.1. Gently transfer the vector solution to a sterilized PCR tube with a P20 pipettor, avoiding bubbles.

2.3.2. Attach a cannula, with the beveled tip facing down, to a vertically oriented stereotaxic holder. Connect a 1 mL Luer-lock syringe to the hypodermic needle hub of the cannula.

2.3.3. Submerge the beveled tip into the vector solution.

NOTE: The syringe should be attached already; attaching it at this point would introduce bubbles into the vector solution.

2.3.4. Apply a gentle negative pressure with the 1 mL syringe to load the solution into the cannula. Visually track the meniscus between the solution and air.

2.3.5. Once the vector solution has been loaded, continue the gentle negative pressure until the solution reaches the needle hub. Remove the 1 mL syringe and inject the colored mineral oil into the hypodermic needle hub.

NOTE: The oil should be injected slowly along the inside wall of the needle hub to form a clear-cut meniscus with the vector solution and to avoid air bubbles.

2.3.6. Attach the hypodermic needle hub to one of the two open ports of a 3-way Luer-lock stopcock.

NOTE: Attaching the hypodermic needle to the closed port will introduce unwanted air behind the oil.

2.3.7. Close the port, fill a 1 mL syringe with air, and then attach it to either of the other two ports. Finally, close the remaining port of the stopcock to connect the syringe to the cannula.

2.3.8. Slowly push air into the cannula. Once the colored oil appears at the tip of the blunt needle in the PTFE tubing, check for air between the solution and the colored oil.

2.3.9. If air is present, apply negative pressure to the syringe to return the colored oil into the needle hub. Remove the bubble and apply positive pressure until a drop of vector solution is visible at the beveled cannula tip.

2.3.10. Close the stopcock to prevent the vector from exiting the cannula by gravity.

## 2.4. Cannula insertion into the target brain area (**Figure 1B**)

2.4.1. Affix the cannula to the stereotaxic manipulator.

2.4.2. To connect the stopcock to the electric air pump, manually transfer the pump tubing (which terminates in a Luer-lock connector) from the non-sterile assistant to the surgeon. The surgeon grasps the Luer-lock connector through the wall of a sterile sleeve, tapes the sleeve tightly around the Luer-lock connector, affixes the stopcock, and then drops the collar of the sleeve, allowing it to extend along the tube by gravity.

2.4.3. Set the air pump to low pressure to test the air pump and cannula. Turn it on and increase the pressure until the oil advances through the cannula and a drop of vector solution is visible at the cannula tip.

2.4.4. Tape a plastic ruler to the PTFE tubing to measure the movement of the meniscus during injection (**Figure 1B,D,F**).

2.4.5. Drive the cannula down with the stereotaxic manipulator and record the depth at which the tip reaches at the surface (dura or pia mater).

2.4.6. Drive the cannula to the deepest site to be injected along the track. The surface will dimple. If injecting the surface cortex, confirm visually that the cannula has penetrated the surface, with a surgical microscope or magnifying loupes if available.

2.4.7. To minimize mistargeting due to tissue compression, drive the cannula in slowly (1 mm/min), quickly (0.5 mm/s) with a 1–5 min wait at the bottom, or overshoot the deepest injection site by 500  $\mu$ m and then retract.

## 2.5. Injection

2.5.1. Inject 0.5  $\mu$ L of the vector with the electric air pump over 10–30 s. Confirm injection flow by tracking the meniscus between the colored oil and the vector solution in the PTFE tube.

2.5.2. Wait for 1 min and retract the cannula to the next injection site along the track.

2.5.3. After the final injection, leave the cannula in place for 10 min to avoid vector efflux.

2.5.4. Retract the cannula and discard it in a biohazard sharps container.

2.5.5. Optionally, inject a small quantity ( $\leq 1 \mu\text{L}$ ) of fluorescent microbeads  $\geq 2 \text{ mm}$  away from the vector injection site to be seen by the eye in unstained tissue and facilitate identification of the injection site for histology.

2.5.6. Repeat this procedure as desired for the other vector solutions at other locations (**Figure 2B**).

## 2.6. Surgery closing

2.6.1. Suture the dura, the muscle, and the skin.

2.6.2. Remove the monkey from the stereotaxic frame and remove all the monitor cables.

2.6.3. Remove the animal from isoflurane anesthesia and extubate following the return of the swallowing reflex.

2.6.4. Provide post-surgical treatment (3–5 days of meloxicam and 7–10 days of cephalexin). Monitor the animals at least once every 10 min until capable of maintaining a stable upright sitting position.

2.6.5. Once fully recovered from anesthesia, reunite animals with cagemates.

## 3. Surgery and AAV vector injection for awake behaving animals (**Figure 1D**)

NOTE: A variant of the technique can be used to make injections into the brains of awake, behaving monkeys, as described below. The neural activity is readily measured in awake behaving animals but can also be measured in some subcortical structures under the anesthesia protocol described here and in some cortical areas with other anesthetic protocols.

### 3.1. Simultaneous injection with recording

3.1.1. To record electrical activity at the injection site, coat the outside of the cannula with epoxy (bottom  $\sim 15 \text{ mm}$ ) and polyimide tubing (remaining length), and then reveal the metal at the tip by scraping the epoxy from it (Injectrode, **Figure 1F**)<sup>2</sup>. Alternatively, insert the cannula and a separate extracellular electrode side-by-side into a double-barreled guide tube (Double-barrel guide tube, **Figure 1E**).

### 3.2. Place the injection cannula at the target brain area.

3.2.1. Place the monkey in the experimental booth, restrict movement of the head, and clean the chamber using standard techniques.

3.2.2. Place and secure a guide tube to the microdrive. Insert the injection cannula into the guide tube.

3.2.3. Advance the cannula until the tip protrudes from the guide tube.

3.2.4. Connect the stopcock to the electric air pump. To confirm proper system function, push a drop of vector solution from the tip using the air pump and confirm movement of the oil-vector solution meniscus.

3.2.5. Withdraw the cannula ~5 mm into the guide tube to protect it. Insert the guide tube into the brain.

3.2.6. Drive the cannula to the site to be injected using the microdrive. Identify the target site by electrical recording (**Figure 2C**) or stimulation.

[Place **Figure 1** here]

[Place **Figure 2** here]

#### **4. Brain tissue processing for histology**

4.1. Wait for 6–8 weeks post-injection to maximize the transgene expression.

NOTE: The optimal duration is dependent on the exact viral vector design utilized for the experiment.

4.2. Process the brain using conventional histological techniques to assess transduction efficiency and selectivity<sup>5–7</sup>.

#### **REPRESENTATIVE RESULTS:**

To demonstrate transgene expression by *in vivo* stereotaxic injection into the NHP brain using the surgical injection method described here, two vectors were selected with enhancers driving expression of the super yellow fluorescent protein-2 (SYFP2) in distinct neuronal types<sup>8,9</sup>. Viral vectors were packaged with the PHP.eB capsid<sup>10</sup>, purified by iodixanol gradient and then concentrated to high titer (>1E13 viral genomes/mL) as measured by qPCR. A volume of 0.5 µL was injected at each of the ten depths along the ten tracks through the cortex for a total injection volume of 5 µL/track in these experiments. **Figure 3A–C** shows the detection of SYFP2 expression using anti-GFP immunostaining 113 days post-injection of the PVALB subclass-specific AAV vector CN2045 into the primary visual cortex region of an adult male *Macaca nemestrina*. The SYFP2 transgene expression is robustly detected in numerous non-pyramidal neurons scattered across the cortical depth, and most SYFP2 expressing neurons were also immunoreactive for PVALB<sup>7</sup>. In contrast, **Figure 3D** shows native SYFP2 expression in the primary motor cortex 64 days post-injection of the L5 neuron subclass-specific AAV vector CN2251. The SYFP2-labeled neurons all exhibit clear pyramidal morphology with somata restricted to L5 and characteristic thick apical



dendrites. These data unambiguously demonstrate precise control of transgene expression in select populations of neocortical neurons in the NHP brain by stereotaxic injection of cell type targeting AAV vectors.

[Place **Figure 3** here]

To demonstrate the utility of this injection technique for neurophysiological and behavioral optogenetic manipulations, three experiments were performed, each on a different monkey (*Macaca mulatta*). In the first experiment (**Figure 4A–D**), AAV vectors carrying the channelrhodopsin-2 transgene (AAV1-hSyn1-ChR2-mCherry) were injected into the left superior colliculus (SC). Every 250  $\mu\text{m}$  at multiple depths of the left SC were injected for a total of 12  $\mu\text{L}$ . In the second experiment (**Figure 4E–G**), 3  $\mu\text{L}$  of AAV1-hSyn-ArchT-EYFP solution was injected into the nucleus reticularis tegmenti pontis (NRTP). In the third experiment (**Figure 4H–K**), 24  $\mu\text{L}$  of AAV9–L7–ChR2–mCherry solution was injected into the cerebellum<sup>6</sup>. After 6–8 weeks of each injection, an optical fiber and a tungsten recording electrode via a double-barrel guide tube was inserted into the brain (**Figure 1G**).

**Figure 4B** shows the response of a superior colliculus (SC) neuron to blue light (450 nm). Continuous light (1.2 s) at 40 mW produced a series of consecutive action potentials (**Figure 4B**, top). Light pulses of 1 ms duration failed to evoke action potentials at 40 mW (**Figure 4B**, middle), but did evoke action potentials reliably at 160 mW, the only other power level tested, with a latency of  $2.7 \text{ ms} \pm 0.6 \text{ ms}$  (**Figure 4B**, bottom). A pulse train (160 mW, frequency: 300 Hz, duty cycle: 15%, duration: 300 ms) evoked saccades consistently with an average latency of  $97 \text{ ms} \pm 32 \text{ ms}$ , a mean amplitude of  $10.4^\circ$  and mean angle of  $47^\circ$  (upward and to the right; **Figure 4C**).

Consistent with studies that modified saccade gain using subthreshold electrical stimulation of the SC<sup>11,12</sup>, optical stimulation of the SC after  $15^\circ$ ,  $18^\circ$ , and  $20^\circ$  left- and downward ( $225^\circ$ ) saccades gradually reduced saccade gain (**Figure 4D**). This gain decrease required  $\sim 250$  trials (green circles) to return to the pre-adaptation gain (black circles), confirming its basis in long-term plasticity.

In the second experiment (**Figure 4E**), the mossy fiber projection was optogenetically suppressed from the nucleus reticularis tegmenti pontis (NRTP) to the oculomotor vermis (OMV) of the cerebellar cortex (lobules VIc and VII). **Figure 4F** shows fluorescently labeled mossy fibers and their rosettes (inset) in the OMV. A yellow laser light (589 nm) was delivered to the OMV via optical fiber and a nearby tungsten electrode was used to record Purkinje cell activity. **Figure 4G** shows simple spike activity before (gray) and after (orange) optogenetic inactivation of NRTP projections (**Figure 4G**, top). Prior to the inactivation, the Purkinje cell exhibited a double burst pattern for  $12^\circ$  rightward saccades (**Figure 4G**, middle, gray). During optogenetic inactivation, the firing rate decreased and changed to a burst-pause pattern (**Figure 4G**, middle, orange). Comparing these two response patterns suggests that the inhibited mossy fiber input to Purkinje cells influences the saccade deceleration phase by driving the second burst (**Figure 4G**, middle, green). The variability of rightward saccades was reduced during optogenetic inactivation,

consistent with the idea that some of the trial-to-trial variability in saccade metrics is due to variability in the signals carried by mossy fibers (**Figure 4G**, bottom, orange).

In the third experiment (**Figure 4H**), Purkinje cells of the OMV were optogenetically stimulated (**Figure 4I**). A train of short light pulses (1.5 ms pulse, 65 mW, 50 Hz) increased the simple spike activity of an isolated Purkinje cell (**Figure 4J**, top). A single 1.5 ms light pulse frequently evoked >1 simple spike action potential (**Figure 4J**, bottom). Optogenetic simple spike activation, timed to occur during a saccade (10 ms long light pulse, 60 mW), increased saccade amplitude (**Figure 4K**), confirming the disinhibitory role of Purkinje cells on the oculomotor burst generator.

[Place **Figure 4** here]

#### **FIGURE AND TABLE LEGENDS:**

**Figure 1: Setup of surgery and apparatus.** (A) Injection cannula. Each part of the cannula is indicated. Inset at bottom-right: magnified picture of cannula tip, scale bar: 500  $\mu$ m. (B) Surgery setup for anesthetized monkeys. The monkey is placed in a stereotaxic frame under a surgical drape. Ventilator (V), intravenous line (IV), blood pressure monitor (BP), and oxygen saturation monitor (O<sub>2</sub>) are connected to the monkey. The injection cannula is inserted into the target area using a stereotaxic micromanipulator. The vector solution is injected by an electric air pump (bottom-left inset, brown) coupled to an air compressor (bottom-left inset, blue). A plastic ruler (top inset) is taped to the PTFE tubing to measure the movement of the meniscus between colored oil (top inset, red) and vector solution (top inset, clear) during injection. (C) Setup to load vector solution into the cannula. (D) A monkey during an injection of vector solution in a neurophysiological booth. The animal's head is held in place by three stabilization-posts, and eye position is recorded by a scleral search coil system. The injection cannula is held and driven to the target depth using a micro-electrode holder/driver. Injection is controlled by monitoring the meniscus between the colored oil and the vector solution through a USB camera (inset picture). (E) Double-barrel guide tube injection. A double-barrel guide tube holder/driver holds an injection cannula and a micro-electrode (see inset). (F) Injectrode. The metal at the tip is exposed by scraping the epoxy coat to provide electrical access to the neurons (inset, scale bar: 500  $\mu$ m). (G) Laser stimulation setup. A double-barrel guide tube holder/driver holds both an optical fiber and a micro-electrode (see inset).

**Figure 2: Diagram of AAV injection sites.** (A) Sagittal section of MR image of the brain showing injection sites in the primary motor cortex and primary visual cortex of a *Macaca nemestrina*. (B) View from the dorsal surface on the corresponding Atlas plate showing cannula placement relative to the central sulcus (primary motor cortex) and primary visual cortex. (C) Unit recording by injectrode. Viral injection and unit recording were conducted in the superior colliculus. The isolated unit before injection (right top) disappeared after the injection (right bottom). (D) Injection track (white arrows). Scale bar: 500  $\mu$ m.

**Figure 3: Example of cell type-specific SYFP2 expression mediated by AAV vectors injected into NHP brain.** (A) Epifluorescence photomicrograph of a fixed brain section from macaque primary visual cortex 113 days post-injection of a PVALB subclass specific AAV vector. Scale bar: 1 mm.

Higher magnification image of the boxed region showing (B) anti-PVALB and (C) overlay of anti-GFP and anti-PVALB signal. Scale bars: 250  $\mu\text{m}$ . (D) Epifluorescence photomicrograph of native SYFP2 fluorescence in a fixed brain slice from macaque primary motor cortex at 64 days post-injection of a layer 5 extratelencephalic subclass specific AAV vector. Scale bar: 500  $\mu\text{m}$ .

**Figure 4: Summary of three optogenetic experiments performed in awake monkeys. (A–D)** Experiment 1, pan-neuronal excitation: viral injection, laser stimulation, and unit recording were conducted in the superior colliculus (A). (B) Representative unit activity evoked by laser stimulation. (C), Horizontal (top) and vertical (middle) components of eye movements and raster plot of unit activity (bottom) evoked by laser stimulation. (D) A representative session of saccade adaptation induced by laser stimulation. Stimulation (100 0.5-ms laser pulses) was delivered 80 ms after each saccade (inset). Saccade gain (saccade amplitude / target amplitude) decreased gradually across trials. (E–G) Experiment 2, pathway-specific inhibition: a viral vector was injected into the nucleus reticularis tegmenti pontis, and laser stimulation (60 mW, continuous) and unit recording were conducted in the oculomotor vermis (E). (F) Histological section of the oculomotor vermis showing labelled mossy fibers (scale bar: 1 mm) and their rosettes (inset, scale bar: 100  $\mu\text{m}$ ). (G) Purkinje cell activity (top: raster, middle: average firing rate) and trajectories of visually guided saccades (bottom) with and without laser stimulation. Grey: laser off trials, orange: laser on trials, green: difference between grey and orange. (H–K) Experiment 3, cell type-specific activation: viral injection, laser stimulation, and unit recording were conducted in the oculomotor vermis (H). (I) Histological section of the oculomotor vermis showing labeled Purkinje cells. Scale bar: 100  $\mu\text{m}$ . (J) Simple spike activity of a Purkinje cell evoked by laser stimulation. Top: raster plot from 14 trials. Bottom: voltage trace from a single representative trial. (K) Trajectories of visually guided saccades with and without laser stimulation. A 10 ms light pulse during saccades increased their amplitudes. Individual saccade trajectories (cyan) and their average (blue) on laser-on trials. Individual saccade trajectories (light grey) and their average (dark grey) on laser-off trials. The light was 450 nm for Experiments 1 and 3 and was 589 nm for Experiment 2.

## DISCUSSION:

Advances in NHP optogenetics have created a need for accurate, reliable intracranial injection methods. Critical steps in this protocol include constructing high-quality cannulas, loading them without introducing bubbles, and selecting injection sites that are not too close together. It is found that injections  $\geq 1$  cm apart usually transduce non-overlapping regions of the cerebral cortex, but this heuristic is dependent on viral serotype, titer, promoter, volume, target, and method of detection. Selecting injection sites that are not directly connected avoids potential confounds produced by opsin trafficking along axons and the propensity that some AAV serotypes have for retrograde transduction.

Advantages of the method described in this report are that it is inexpensive, uses sterilizable and disposable components, and has the ability to target diverse brain areas of any depth. It also permits control of injection speed and volume by virtue of the speed with which the air valve can be controlled. Air pressure can be increased transiently to dislodge a clog and then reduced quickly to avoid subsequent over-injection that would be produced by sustained pressure as is

433 produced by some mechanical pumps. Disposable components reduce the risk of cross-  
434 contamination between injection sites.

435  
436 The method can be used to inject NHPs while anesthetized and in a stereotaxic frame (**Figure 3**)  
437 or alert and head-fixed (**Figure 4**). The former has the advantage of allowing injections to be  
438 targeted in stereotaxic coordinates, and it allows visual confirmation of cannula penetration  
439 through an acute durotomy (incising the dura in an awake monkey, through a chronic  
440 craniotomy, has a high risk of infection). The latter approach has the advantages of reducing the  
441 number of survival surgeries and therefore the stress to the animal, being compatible with  
442 electrophysiological recordings during behavior, and using the same coordinate frame and  
443 instrumentation used to insert optical fibers for post-injection experiments. The injection  
444 technique in awake monkeys could be further improved by making injections through artificial  
445 dura<sup>13–15</sup>. This would confer the additional advantages of direct visualization of injection sites and  
446 the subsequent tissue fluorescence that indicates successful transduction.

447  
448 Several other AAV injection techniques have been used in NHPs. Recently, a multi-channel  
449 injection device was developed to deliver AAV vectors uniformly to large NHP cortical regions<sup>16</sup>.  
450 Similar results can be obtained using convection-enhanced delivery<sup>17,18</sup>. These methods aim to  
451 maximize transduction spread—an important goal, but one that is distinct from the spatial  
452 precision our method aims to achieve.

453  
454 An alternative method used in the past, injected AAV vectors through a length of borosilicate  
455 tubing that is beveled to a sharp tip on one end and attached to a Hamilton syringe on the  
456 other<sup>5,6</sup>. This method has much in common with the method described in this paper. The viral  
457 vector is held in a length of tubing, the space in the tubing behind the virus is filled with dyed oil,  
458 and flow of the virus is monitored via the movement of the oil-virus meniscus. This alternative  
459 technique requires less equipment and preparation, but it requires drawing oil into the  
460 borosilicate tubing through the beveled tip by negative pressure and loading the vector via the  
461 same route subsequently. This inevitably results in traces of oil delivered to the brain.  
462 Additionally, in our experience, the borosilicate tubing must have a diameter of ~350  $\mu\text{m}$  to  
463 penetrate dura even when beveled and therefore causes greater mechanical damage than the  
464 thinner metal cannula described in this report (**Figure 2D**). 30 G tubing was used because its  
465 critical buckling load is high enough to mediate dura penetration despite a 1–10 cm length,  
466 because it fits the Teflon tubing tightly, and because it rarely clogs. 33 G tubing was used for  
467 injection when tissue damage was particularly concerning but found that it clogs and bends more  
468 easily and is more difficult to mate with the PTFE tubing. 36 G is not stiff enough to penetrate  
469 dura mater.

470  
471 A second alternative injection technique is to mate the output of the picopump to a back of a  
472 vector-loaded, pulled-glass pipette<sup>19</sup>. The vector is forced from the pipette tip by direct,  
473 intermittent pressure from the picopump, eliminating the need for oil. Similar to the single-tube  
474 method explained above, the lack of any material junctions between the meniscus and the  
475 cannula tip reduces the risk of leaks. However, the sharp taper and delicate tips of glass pipettes  
476 prevent them from penetrating NHP dura or targeting deep structures.

**ACKNOWLEDGMENTS:**

This study was supported by WaNPRC/ITHS P51OD010425 (JTT), National Institute of Health (NIH) grants EY023277 (R01 for YK), EY030441 (R01 for GH), MH114126 (RF1 to JTT, Boaz Levi, Ed Lein), EY028902 (R01 for RS), and made possible by NIH grants OD010425 (P51 for WaNPRC) and University of Washington Royalty Research Fund A148416. The authors would like to thank Yasmine El-Shamayleh and Victoria Omstead for histology, Refugio Martinez for viral vector cloning, Shane Gibson for AAV vector purification and titer determination, and John Mich for assistance with NHP brain tissue processing.

**DISCLOSURES:**

The authors have nothing to disclose.

**REFERENCES:**

1. Kojima, Y., Robinson, F. R., Soetedjo, R. Cerebellar fastigial nucleus influence on ipsilateral abducens activity during saccades. *Journal of Neurophysiology*. **111** (8), 1553–1563 (2014).
2. Kojima, Y., Soetedjo, R. Elimination of the error signal in the superior colliculus impairs saccade motor learning. *Proceedings of the National Academy of Sciences of the United States of America*. **115** (38), E8987–E8995 (2018).
3. Kojima, Y., Soetedjo, R., Fuchs, A. F. Effects of GABA agonist and antagonist injections into the oculomotor vermis on horizontal saccades. *Brain Research*. **1366**, 93–100 (2010).
4. Kojima, Y., Soetedjo, R., Fuchs, A. F. Effect of inactivation and disinhibition of the oculomotor vermis on saccade adaptation. *Brain Research*. **1401**, 30–39 (2011).
5. De, A., El-Shamayleh, Y., Horwitz, G. D. Fast and reversible neural inactivation in macaque cortex by optogenetic stimulation of GABAergic neurons. *eLife*. **9**, e52658 (2020).
6. El-Shamayleh, Y., Kojima, Y., Soetedjo, R., Horwitz, G. D. Selective optogenetic control of purkinje cells in monkey cerebellum. *Neuron*. **95** (1), 51–62.e4 (2017).
7. Mich, J. K. et al. Functional enhancer elements drive subclass-selective expression from mouse to primate neocortex. *Cell Reports*. **34** (13), 108754 (2021).
8. Graybuck, L. T. et al. Enhancer viruses for combinatorial cell subclass-specific labeling. *Neuron*. S0896–6273 (21) 00159-8 (2020).
9. Michel, J., Benninger, D., Dietz, V., van Hedel, H. J. Obstacle stepping in patients with Parkinson's disease. Complexity does influence performance. *Journal of Neurology*. **256** (3), 457–463 (2009).
10. Chan, K. Y. et al. Engineered AAVs for efficient noninvasive gene delivery to the central and peripheral nervous systems. *Nature Neuroscience*. **20** (8), 1172–1179 (2017).
11. Kaku, Y., Yoshida, K., Iwamoto, Y. Learning signals from the superior colliculus for adaptation of saccadic eye movements in the monkey. *Journal of Neuroscience*. **29** (16), 5266–5275 (2009).
12. Soetedjo, R., Fuchs, A. F., Kojima, Y. Subthreshold activation of the superior colliculus drives saccade motor learning. *Journal of Neuroscience*. **29** (48), 15213–15222 (2009).
13. Kleinbart, J. E. et al. A modular implant system for multimodal recording and manipulation of the primate brain. *Annual International Conference of the IEEE Engineering in Medicine and*

520 *Biology Society. IEEE Engineering in Medicine and Biology Society. Annual International*  
521 *Conference. 2018, 3362–3365 (2018).*

522 14. Arieli, A., Grinvald, A., Slovin, H. Dural substitute for long-term imaging of cortical activity  
523 in behaving monkeys and its clinical implications. *Journal of Neuroscience Methods. 114* (2), 119–  
524 133 (2002).

525 15. Ruiz, O. et al. Optogenetics through windows on the brain in the nonhuman primate.  
526 *Journal of Neurophysiology. 110* (6), 1455–1467 (2013).

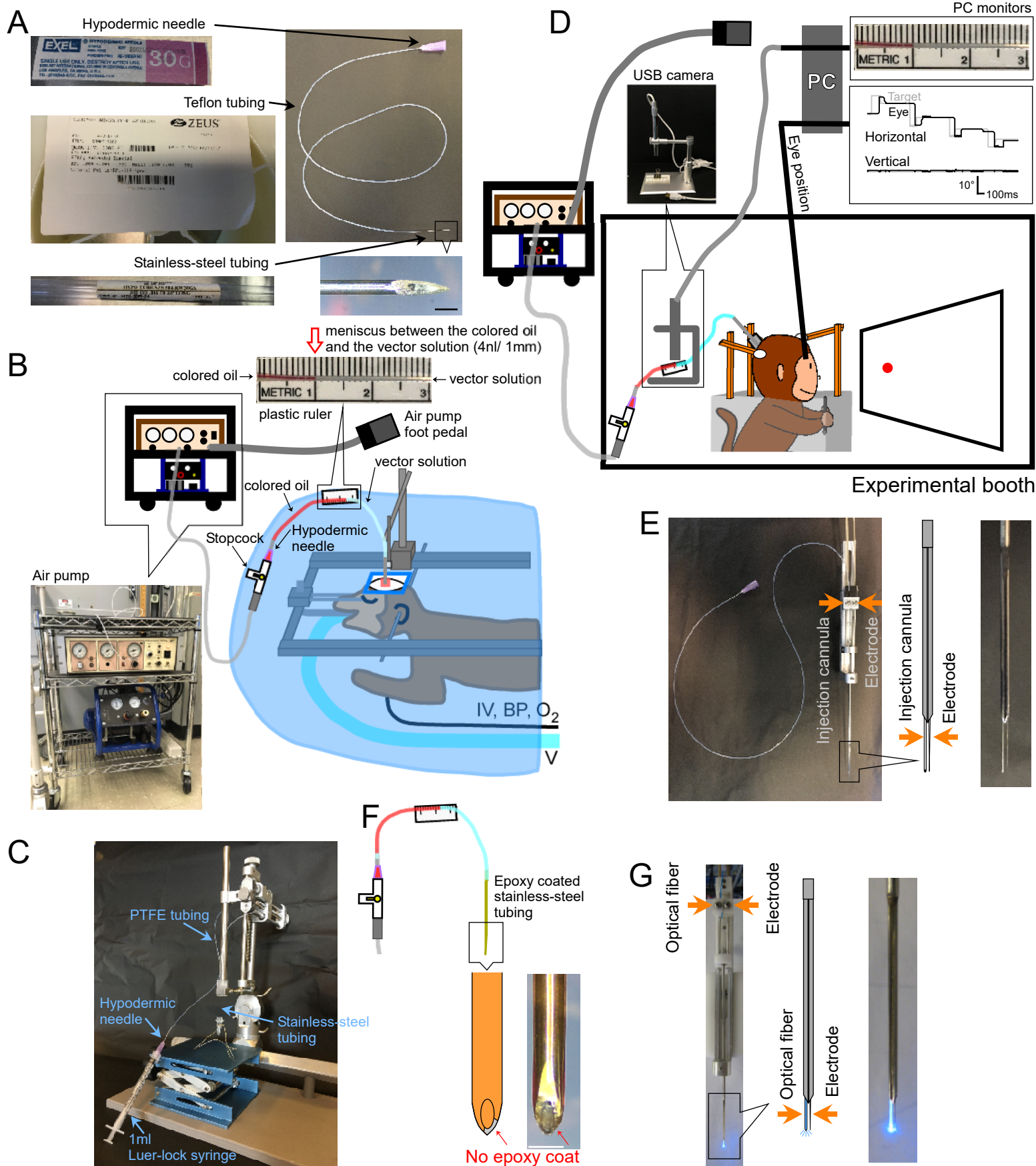
527 16. Fredericks, J. M. et al. Methods for mechanical delivery of viral vectors into rhesus  
528 monkey brain. *Journal of Neuroscience Methods. 339*, 108730 (2020).

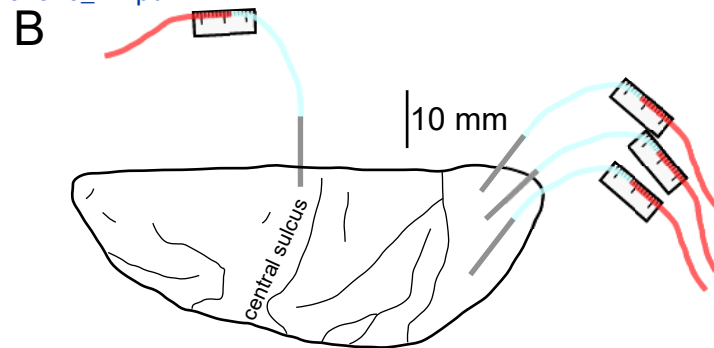
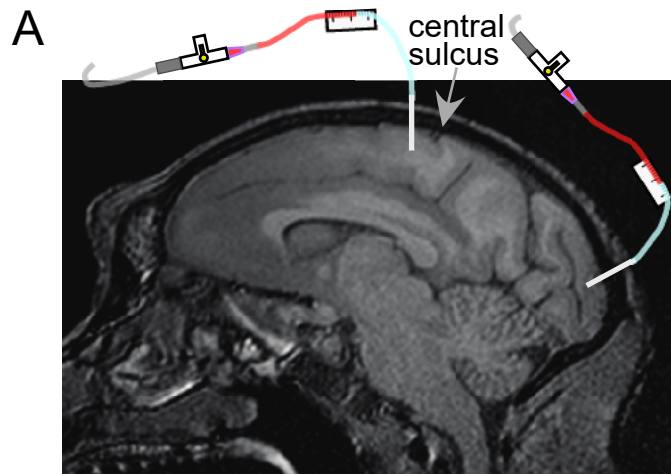
529 17. Bankiewicz, K. S. et al. Convection-enhanced delivery of AAV vector in parkinsonian  
530 monkeys; in vivo detection of gene expression and restoration of dopaminergic function using  
531 pro-drug approach. *Experimental Neurology. 164* (1), 2–14 (2000).

532 18. Yazdan-Shahmorad, A. et al. Widespread optogenetic expression in macaque cortex  
533 obtained with MR-guided, convection enhanced delivery (CED) of AAV vector to the thalamus.  
534 *Journal of Neuroscience Methods. 293*, 347–358 (2018).

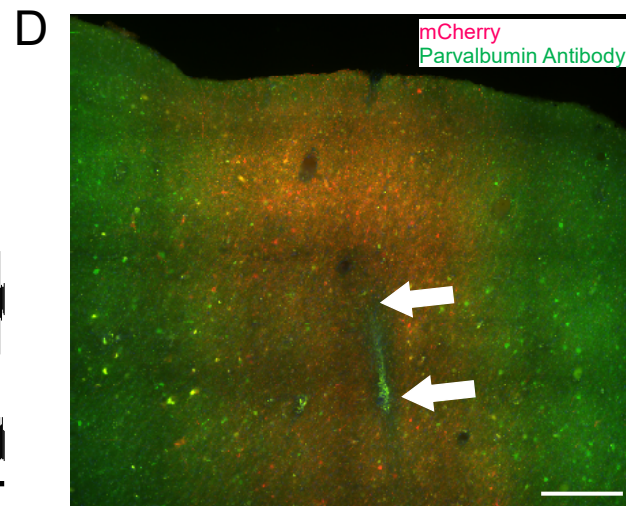
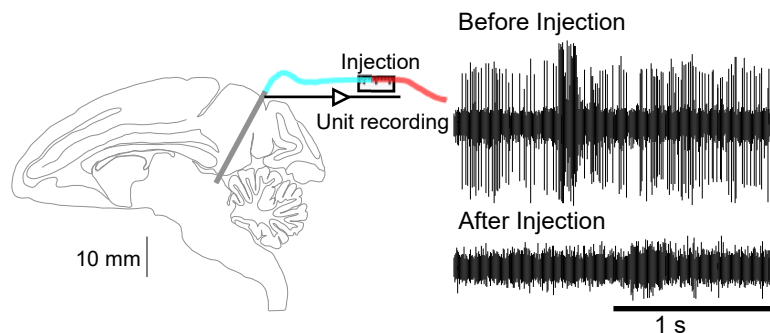
535 19. Nathanson, J. L., Yanagawa, Y., Obata, K., Callaway, E. M. Preferential labeling of inhibitory  
536 and excitatory cortical neurons by endogenous tropism of adeno-associated virus and lentivirus  
537 vectors. *Neuroscience. 161* (2), 441–450 (2009).

538

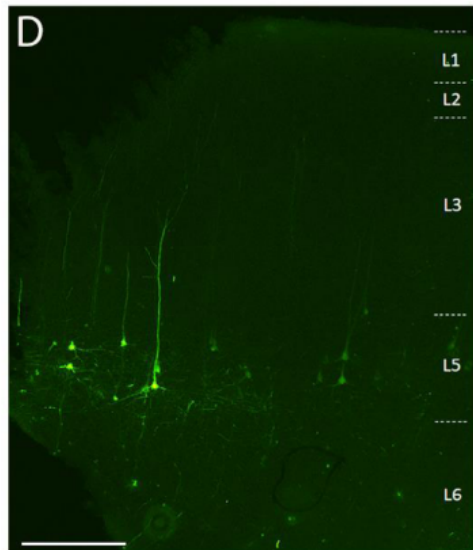
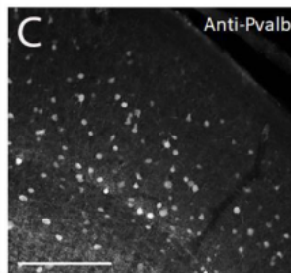
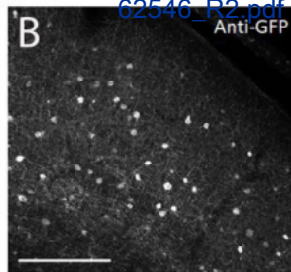
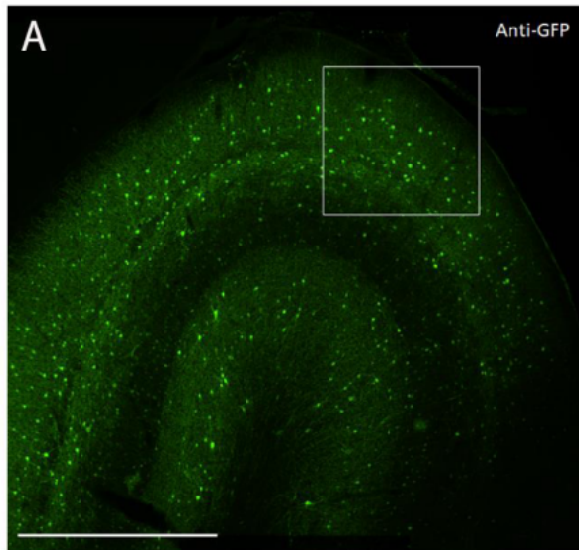


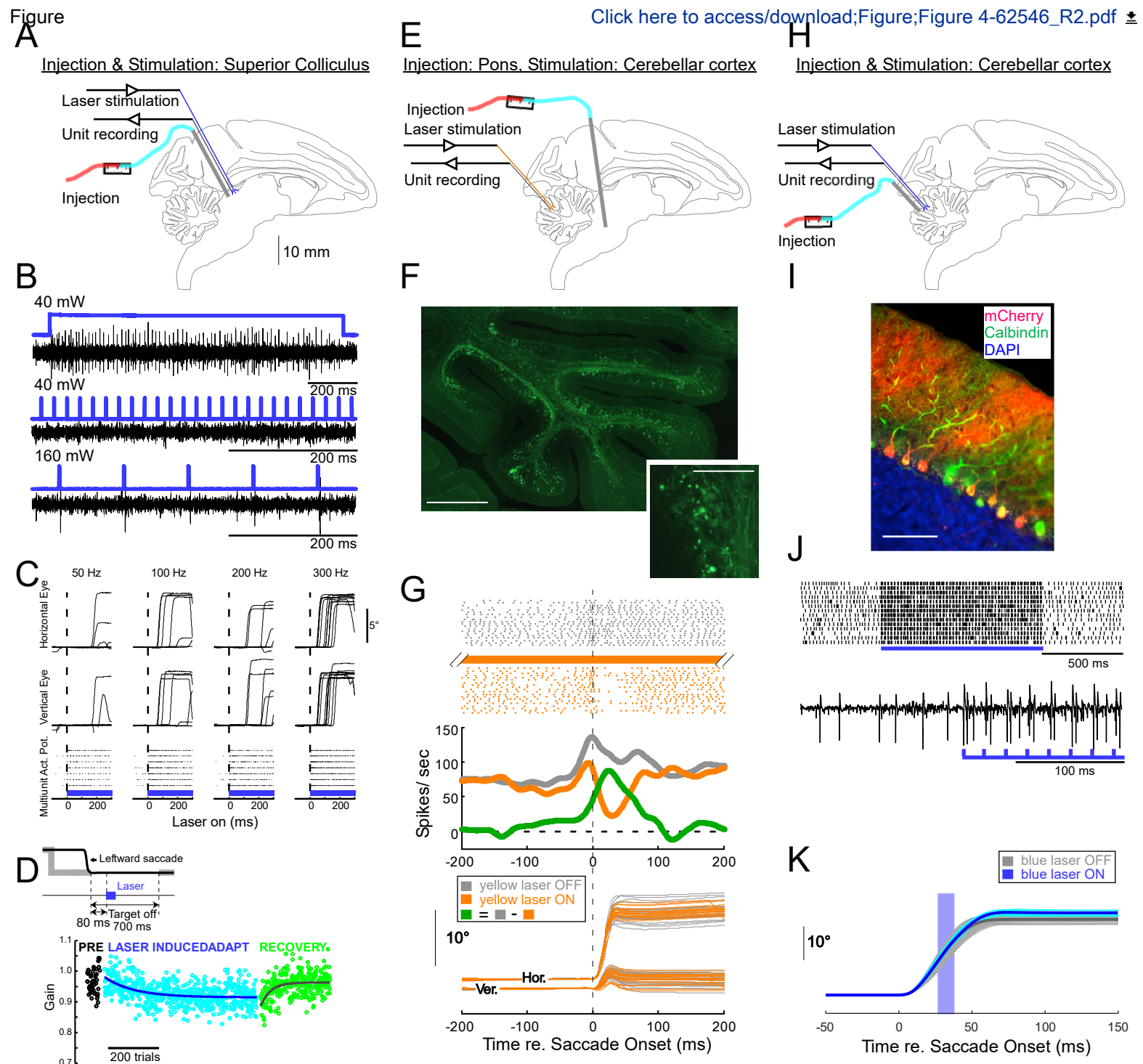


**C** Injection & recording: Superior Colliculus









Equipment	Item	Company
Stereotaxic set	Allen keys	BONDHUS
	Cannula holder	KOPF
	Carrier (manipulator)	KOPF
	Carrier platform	KOPF
	Carrier stand	KOPF
	Eye, ear, mouth bars	KOPF
	Stereotaxic base	KOPF
Cannula	1 mL Luer-lock syringes	BD
	Cannulas*	(homemade - see below)
	Colored oil**	(homemade - see below)
	Elevator (for tube rack)	Cole-Parmer
	Filter tip	Genesee Scientific
	Fluorescent microbeads	Lumafluor
	P20 pipetman	Gilson
	PCR tubes	Olympus Plastics
	Stopcock	Cole-Parmer
	Tube rack	homemade
	Vector solution	(homemade)
Electric air pump set	Electric air pump	World Precision Instruments
	Foot pedal	World Precision Instruments
	Tube cover	EZ Drape
General surgery tools	Beaker	MEDLINE
	Burrs	STRYKER
	Double pronged tissue pick	Fine Science Tools
	Drapes	MEDLINE
	Dressing forceps	Miltex
	Drill	STRYKER
	Drill bits	STRYKER
	Gauze	MEDLINE
	Hemostatic mosquito forceps	Miltex
	Light handles	SKYTRON
	Needle holder	Miltex
	Periosteal elevator	Miltex
	Rongeurs	Miltex
	Saline	BAXTER
	Scalpel	Bard-Parker

	Scissors	Miltex
	Senn retractors	Miltex
	Sterile gloves	MEDLINE
	Suction	medela
	Suction tip	MEDLINE
	Suction tube	COVIDEN
	Surgical gowns	MEDLINE
	Surgical pens & ruler	MEDLINE
	Suture	COVIDEN
	Tissue forceps	Miltex
	Towel clamps	Miltex
	Wood swabs	MEDLINE
*cannulas	Hypodermic needle	EXELINT INTERNATIONAL
	Stainless steel tube	K-TUBE
	PTFE tube	ZEUS
**colored oil	Liquid Candle Dye Concentrate	PremiumCraft
	Mineral oil	Vi-Jon
		STE

Product	Comment (sterilization method)
10936	STERRAD
1770	STERRAD
1404	STERRAD
1430	NA
1449	STERRAD
1430	NA
1210	NA
309628	NA (sterilized package)
NA	steam (autoclave)
NA	NA
UX-08057-10	STERRAD
23-404	NA (sterilized package)
R170	NA
FA10003M	NA
22-161	STERRAD
3060004	STERRAD
NA	STERRAD
NA	NA
PV830	NA
3260	NA
A400-1000	NA (sterilized package)
azlon	STERRAD
277-10-235	STERRAD
18067-11	STERRAD
DYNJP3004	NA (sterilized package)
6-118	STERRAD
Q9R-5400	NA
277-82-87	STERRAD
NON26334	NA (sterilized package)
7-2, 7-4	STERRAD
Stellar XL	STERRAD
8-2	STERRAD
18-1968	STERRAD
17-4800	STERRAD
2F7122	STERRAD
372610	STERRAD

5-12, 5-114	STERRAD
28065	STERRAD
Triumph Micro	NA (sterilized package)
200-4869	NA
DYNDFR12S	NA (sterilized package)
8888301614	NA (sterilized package)
DYNJP2002S	NA (sterilized package)
DYNJSM03	NA (sterilized package)
SL-635	NA (sterilized package)
6-114	STERRAD
7-504	STERRAD
MDS202095	NA (sterilized package)
26437	NA (sterilized package)
K30R	NA
216200	NA
Red/Pink	NA
S0883	NA

RRAD: low-temperature hydrogen peroxide gas plasma

Editorial comments:

1. Lines 77-78/ 83-99: Please present the animal protocol as numbered steps with the rest of the protocol.

[Done.](#)

2. Please add a note at the beginning of the protocol stating that the protocol will be presented on an agar cube instead of an animal sample (Reviewer #1 major concern 4). As the authors prefer to present a mock experiment instead of inserting the cannula into the brain, please revise the protocol to be more explicit about using agar block. Please add the necessary protocol steps to explain the insertion of the cannula into the agar block.

[We changed our plan – we will present the protocol on a monkey brain as described in the manuscript, not on an agar block.](#)

3. Figure 1B: Please revise the text in the figure to “4 nL/ 1 mm” instead of “4nl/1 mm”

[Done.](#)

4. Figure 2: Please maintain a single space between the numeral and (abbreviated) unit. Revise “10mm” to “10 mm” (Figure 2B, C). Please use standard abbreviations for time units (revise “1 sec” to “1 s”) (Figure 2C).

[Done.](#)

5. Figure 4: Please maintain a single space between the numeral and (abbreviated) unit (e.g., “10 mm”, “200 ms”, “200 Hz”, “40 mW”, “Spikes/s”, etc.) (Figure 4A, B, C, D, G, J).

[Done.](#)

TITLE: (150-character maximum):

Injections of AAV vectors for optogenetics in anesthetized and awake behaving non-human primate brain

AUTHORS AND AFFILIATIONS:

Yoshiko Kojima

Dept. of Otolaryngology – Head and Neck Surgery, University of Washington, Seattle WA USA.

Washington National Primate Research Center, University of Washington, Seattle WA USA.

ykojima@uw.edu

Jonathan T. Ting

Allen Institute for Brain Science, Seattle WA USA.

Washington National Primate Research Center, University of Washington, Seattle WA USA.

Dept. of Physiology & Biophysics, University of Washington, Seattle WA USA.

JonathanT@alleninstitute.org

Robijanto Soetedjo

Dept. of Physiology & Biophysics, University of Washington, Seattle WA USA.

Washington National Primate Research Center, University of Washington, Seattle WA USA.

robi@uw.edu

Shane D. Gibson

Washington National Primate Research Center, University of Washington, Seattle WA USA.

sgibso@uw.edu

Gregory D. Horwitz

Dept. of Physiology & Biophysics, University of Washington, Seattle WA USA.

Washington National Primate Research Center, University of Washington, Seattle WA USA.

ghorwitz@uw.edu

Corresponding: Yoshiko Kojima

KEYWORDS: (6 minimum, 12 maximum)

Channelrhodopsin-2, AAV, Cerebellum, neocortex, Surgery, Cannula, Enhancers

SUMMARY: (10-word minimum, 50-word maximum)

As currently implemented, optogenetics in non-human primates requires injection of viral vectors into the brain. An optimal injection method should be reliable and, for many applications, capable of targeting individual sites of arbitrary depth that are readily and unambiguously identified in postmortem histology. An injection method with these properties is presented.

ABSTRACT: (150-word minimum, 300-word maximum)

Optogenetic techniques have revolutionized neuroscience research and are poised to do the same for gene therapy for neurological disorders. The clinical use of optogenetics, however, requires that safety and efficacy are demonstrated in animal models, ideally non-human primates (NHPs) because of their neurological similarity to humans. The number of candidate vectors that are potentially useful for neuroscience and medicine is vast, and no high throughput means to test these vectors yet exists. Thus, there is a need for techniques to make multiple spatially and



volumetrically accurate injections of viral vectors into NHP brain that can be identified unambiguously through postmortem histology. Described herein is such a method. Injection cannulas are constructed from polytetrafluoroethylene (PTFE) tubing coupled to beveled, stainless-steel tubes. These cannulas are autoclavable, disposable, and have low minimal loading volumes, making them ideal for the injection of expensive, highly concentrated viral vector solutions. An inert red-dyed mineral oil fills the dead space and forms a visible meniscus with the vector solution, allowing instantaneous and accurate measurement of injection rates and volumes. The oil is loaded into the rear of the cannula, reducing the risk of co-injection with the vector. Cannulas can be loaded in 10 minutes and injections can be made in 20 minutes. This procedure is well suited for injection in awake, behaving or anesthetized animals. When used to deliver high-quality viral vectors, this procedure can produce robust expression of optogenetic proteins, allowing optical control of neural activity and behavior in NHPs.

INTRODUCTION: (150-word minimum, 1,500-word maximum, 2-paragraph minimum)

Optogenetics in non-human primates (NHPs) typically involves the injection of viral vectors directly into the brain. One class of vectors that is well suited for this application are those based on adeno-associated virus (AAV). These vectors consist of a protein capsid surrounding a single-stranded DNA genome that, in turn, consists of a promoter, an opsin gene, and optionally other protein-coding and gene-regulatory elements. Advances in molecular cloning and cell culture techniques have facilitated the manipulation and combination of these components for the development of new vectors. Consequently, the collection of AAV vectors that is potentially useful for NHP optogenetics is large and growing rapidly.

At present, the utility of an AAV vector for NHP optogenetics requires testing in vivo. This fact is a substantial barrier to progress. Animals must be used sparingly, and testing multiple vectors in a single animal requires that injection sites be positioned judiciously relative to neural architecture and well separated relative to viral spread. Accurate histological assessment requires that injections are spatially and volumetrically accurate. To make such injections, we adapted and simplified an injection technique which we have used previously for focal delivery of pharmacological agents<sup>1-4</sup>. This injection technique is inexpensive, uses disposable, sterilizable components, can be used in anesthetized or awake behaving monkeys, and can be used to target diverse brain areas of any depth. The following protocol describes step-by-step procedures for fabricating the disposable components and making the surgical injections in the NHP brain. Advantages and disadvantages of the technique are discussed.

PROTOCOL: (1-page minimum, 10-page maximum), highlight in yellow up to 3 pages to be featured in the video

All experiments were performed in accordance with the Guide for the Care and Use of Laboratory Animals and exceeded the minimal requirements recommended by the Institute of Laboratory Animal Resources and the Association for Assessment and Accreditation of Laboratory Animal Care International. All the procedures were evaluated and approved by the Animal Care and Use Committee of the University of Washington (UW IACUC protocol #4167-01). Sterile instruments and technique were used throughout all surgical procedures.

## 1. Making a cannula (Fig. 1A)

### 1.1) Preparation of each part

#### 1.1.1) Hypodermic needle (30 gauge, 13 mm length)

Blunt the needle tip with a disk grinder.

#### 1.1.2) Stainless-steel tubing (30-gauge, inside diameter=0.16 mm, outside diameter=0.31 mm)

Cut stainless-steel tubing to a length tailored to the depth of the target brain area (25 mm is well suited to inject the dorsal surface of the cerebral cortex). With a disk grinder, bevel one end of the cut tube and smooth the other. Deburr the inside of the tube with a broach.

#### 1.1.3) PTFE tubing (inside diameter=0.23 ± 0.02 mm, wall=0.23 ± 0.02 mm, 1 mm corresponds to 42 ± 7 nL of fluid)

Cut the PTFE tubing to a length appropriate for the amount of vector solution to load (1  $\mu$ l of vector solution occupies 24 mm of tubing). Flare both ends of the PTFE tube by insertion of the blunted hypodermic needle.

### 1.2) Assembly (Fig. 1A)

Insert the blunted hypodermic needle approximately 5 mm into one end of the PTFE tube. Insert the unbeveled end of the stainless-steel tubing approximately 5 mm into the other end.

### 1.3) Pre-injection testing

Inject filtered water through the hypodermic needle hub of the cannula. Confirm that water exits the beveled stainless-steel tubing tip smoothly and that water does not leak from either junction.

## 2. Injection procedure for anesthetized animals

### 2.1) Surgery preparation

Sterilize surgical instruments and supplies using the procedures in TABLE OF MATERIALS. If needed, take a head MRI for targeting deep brain structures (Fig. 2A). Immediately before surgery, sedate animals with ketamine (10-15 mg/kg) and administer antibiotics (cefazolin) and analgesics (sustained-release buprenorphine and meloxicam) intramuscularly. Then deliver propofol via intravenous (IV) catheter in the saphenous or cephalic veins. Intubate and transit the animal onto isoflurane gas. Confirm proper anesthetization by stable heart rate, blood pressure, and respiratory rate, relaxed skeletal muscles, and the absence of palpebral or withdrawal reflexes. Apply artificial tear ointment to the corneas to prevent drying.

### 2.2) Injection area preparation

Incise skin and reflect muscle.

Place the manipulator on the stereotaxic frame, position it so that it is aimed at the target brain area, and mark craniotomy position on the skull with a sterilized pen.

Remove the stereotaxic manipulator and perform the craniotomy. Incise dura if desired (e.g. to visualize sulcal landmarks).

Return the manipulator to the stereotaxic frame.

### 2.3) Vector solution loading (Fig. 1C)

With a P20 pipettor, gently transfer the vector solution to a sterilized PCR tube, avoiding bubbles.

Attach a cannula, with the beveled tip facing down, to a vertically oriented stereotaxic holder.

Connect a 1 ml Luer-lock syringe to the hypodermic needle hub of the cannula.

Submerge the beveled tip into the vector solution. Note that the syringe should be attached already; attaching it at this point would introduce bubbles into the vector solution.

Apply gentle negative pressure with the 1 ml syringe to load the solution into the cannula. Visually track the meniscus between the solution and air.

Once the vector solution has been loaded, continue the gentle negative pressure until the solution reaches the needle hub. Remove the 1 ml syringe and inject colored mineral oil into the hypodermic needle hub. Note that the oil should be injected slowly along the inside wall of the needle hub to form a clear-cut meniscus with the vector solution and to avoid air bubbles.

Attach the hypodermic needle hub to one of the two open ports of a 3-way Luer-lock stopcock. Note that attaching it to the closed port would introduce unwanted air behind the oil. Close the port, fill a 1 ml syringe with air, and attach it to either of the other two ports. Finally, close the remaining port of the stopcock to connect the syringe to the cannula.

Slowly push air into the cannula. Once the colored oil appears at the tip of the blunt needle in the PTFE tubing, check for air between the solution and the colored oil. If air is present, apply negative pressure to the syringe to return the colored oil into the needle hub, remove the bubble, and apply positive pressure until a drop of vector solution is visible at the beveled cannula tip.

Close the stopcock to prevent the vector from exiting the cannula by gravity.

#### 2.4) Cannula insertion into the target brain area (Fig. 1B)

Affix the cannula to the stereotaxic manipulator.

Connect the stopcock to the electric air pump by manually transferring the pump tubing (which terminates in a Luer-lock connector) from the non-sterile assistant to the surgeon. The surgeon grasps the Luer-lock connector through the wall of a sterile sleeve, tapes the sleeve tightly around the Luer-lock connector, affixes the stopcock, and drops the collar of the sleeve, allowing it to extend along the tube by gravity.

Test the air pump and cannula by setting the air pump to low pressure, turning it on, and increasing the pressure until the oil advances through the cannula and a drop of vector solution is visible at the cannula tip.

Tape a plastic ruler to the PTFE tubing to measure the movement of the meniscus during injection (Fig. 1B, 1D, 1F).

Drive the cannula down with the stereotaxic manipulator and record the depth at which the tip reaches at the surface (dura or pia mater).

Drive the cannula to the deepest site to be injected along the track. The surface will dimple. If injecting surface cortex, confirm visually that the cannula has penetrated the surface, with a surgical microscope or magnifying loupes if available. To minimize mistargeting due to tissue compression, drive the cannula in slowly (1 mm/min), quickly (0.5 mm/sec) with a 1-5 minute wait at the bottom, or overshoot the deepest injection site by 500  $\mu$ m and then retract.

#### 2.5) Injection

Inject 0.5  $\mu$ l of vector with the electric air pump over 10–30 s. Confirm injection flow by tracking the meniscus between the colored oil and the vector solution in the PTFE tube.

Wait 1 minute and retract the cannula to the next injection site along the track.

After the final injection, leave the cannula in place for 10 mins to avoid vector efflux.

Retract the cannula and discard it in a biohazard sharps container.

Optionally, inject a small quantity ( $\leq 1 \mu$ l) of fluorescent microbeads  $\geq 2$  mm away from the vector injection site. The beads can be seen by eye in unstained tissue and facilitate identification of the injection site for histology.

Repeat this procedure as desired for the other vector solutions at other locations (Fig. 2B).

#### 2.6) Surgery closing

Suture dura, muscle, and skin. Remove the monkey from the stereotaxic frame and remove all monitor cables. Remove the animal from isoflurane anesthesia and extubate following return of the swallowing reflex. Provide post-surgical treatment (3–5 days of meloxicam and 7-10 days of cephalexin). Monitor animals at least once every ten minutes until capable of maintaining a stable upright sitting position. Once fully recovered from anesthesia, reunite animals with cagemates.

### 3. Surgery and AAV vector injection for awake behaving animals (Fig. 1D)

A variant of the technique can be used to make injections can be made into the brains of awake, behaving monkeys, as described below. Note that neural activity is readily measured in awake behaving animals but can also be measured in some subcortical structures under the anesthesia protocol described here and in some cortical areas with other anesthetic protocols.

#### 3.1) Simultaneous injection with recording

To record electrical activity at the injection site, coat the outside of the cannula with epoxy (bottom ~15 mm) and polyimide tubing (remaining length), and reveal the metal at the tip by scraping the epoxy from it (Injectrode, Fig. 1F)<sup>2</sup>. Alternatively, insert the cannula and a separate extracellular electrode side-by-side into a double-barreled guide tube (Double-barrel guide tube, Fig. 1E).

### 3.2) Place the injection cannula at target brain area

Place the monkey in the experimental booth, restrict movement of the head, and clean the chamber using standard techniques.

Place and secure a guide tube to the microdrive.

Insert the injection cannula into the guide tube.

Advance the cannula until the tip protrudes from the guide tube.

Connect the stopcock to the electric air pump. To confirm proper system function, push a drop of vector solution from the tip using the air pump and confirm movement of the oil-vector solution meniscus.

Withdraw the cannula ~5 mm into the guide tube to protect it.

Insert the guide tube into the brain.

Drive the cannula to the site to be injected using the microdrive. The target site can be identified by electrical recording (Fig. 2C) or stimulation.

Fig. 1 Setup of surgery and apparatus. A, Injection cannula. Each part of the cannula is indicated. Inset at bottom-right: magnified picture of cannula tip, scale bar: 500  $\mu$ m. B, Surgery setup for anesthetized monkeys. The monkey is placed in a stereotaxic frame under a surgical drape. Ventilator(V), intravenous line (IV), blood pressure monitor (BP), and oxygen saturation monitor (O2) are connected to the monkey. The injection cannula is inserted into the target area using a stereotaxic micromanipulator. The vector solution is injected by an electric air pump (bottom-left inset, brown) coupled to an air compressor (bottom-left inset, blue). A plastic ruler (top inset) is taped to the PTFE tubing to measure the movement of the meniscus between colored oil (top inset, red) and vector solution (top inset, clear) during injection. C, Setup to load vector solution into the cannula. D, A monkey during an injection of vector solution in a neurophysiological booth. The animal's head is held in place by 3 stabilization-posts, and eye position is recorded by a scleral search coil system. The injection cannula is held and driven to the target depth using a micro-electrode holder/driver. Injection is controlled by monitoring the meniscus between the colored oil and the vector solution through a USB camera (inset picture). E, Double-barrel guide tube injection. A double-barrel guide tube holder/driver holds an injection cannula and a micro-electrode (see inset). F, Injectrode. The metal at the tip is exposed by scraping the epoxy coat to provide electrical access to the neurons (inset, scale bar: 500  $\mu$ m). G, Laser stimulation setup. A double-barrel guide tube holder/driver holds both an optical fiber and a micro-electrode (see inset).

Fig. 2 Diagram of AAV injection sites. A, Sagittal section of MR image of the brain showing injection sites in the primary motor cortex and primary visual cortex of a *Macaca nemestrina*. B, View from the dorsal surface on the corresponding Atlas plate showing cannula placement relative to the central sulcus (primary motor cortex) and primary visual cortex. C, Unit recording by injectrode. Viral injection and unit recording were conducted in the superior colliculus. The isolated unit before injection (right top) disappeared after the injection (right bottom). D, Injection track (white arrows). Scale bar: 500  $\mu$ m.

### 4. Brain tissue processing for histology

Wait 6-8 weeks post-injection to maximize transgene expression. Note that the optimal duration is dependent on the exact viral vector design utilized for the experiment. **Anesthetize animals deeply and humanely euthanize with sodium pentobarbital.** Process the brain using conventional histological techniques to assess transduction efficiency and selectivity<sup>5-7</sup>.

## REPRESENTATIVE RESULTS:

Five healthy macaques (2 *Macaca mulatta*, 3 *Macaca nemestrina*. Male. 4-11 years old) participated in this study.

### 1. Cell type-specific transgene expression with AAV vectors

To demonstrate transgene expression by in vivo stereotaxic injection into the NHP brain using the surgical injection method described here, we selected two vectors with enhancers driving expression of the super yellow fluorescent protein-2 (SYFP2) in distinct neuronal types<sup>8,9</sup>. Viral vectors were packaged with the PHP.eB capsid<sup>10</sup>, purified by iodixanol gradient and concentrated to high titer ( $>1E13$  viral genomes/mL) as measured by qPCR. We injected 0.5  $\mu$ L at each of 10 depths along 10 tracks through the cortex for a total injection volume of 5  $\mu$ L/track in these experiments. Fig. 3A-C shows the detection of SYFP2 expression using anti-GFP immunostaining 113 days post-injection of the PVALB subclass-specific AAV vector CN2045 into the primary visual cortex region of an adult male *Macaca nemestrina*. The SYFP2 transgene expression is robustly detected in numerous non-pyramidal neurons scattered across the cortical depth, and most SYFP2 expressing neurons were also immunoreactive for PVALB<sup>7</sup>. In contrast, Fig. 3D shows native SYFP2 expression in the primary motor cortex 64 days post-injection of the L5 neuron subclass-specific AAV vector CN2251. The SYFP2-labeled neurons all exhibit clear pyramidal morphology with somata restricted to L5 and characteristic thick apical dendrites. These data unambiguously demonstrate precise control of transgene expression in select populations of neocortical neurons in the NHP brain by stereotaxic injection of cell type targeting AAV vectors.

Fig. 3 Example of cell type-specific SYFP2 expression mediated by AAV vectors injected into NHP brain. A, Epifluorescence photomicrograph of a fixed brain section from macaque primary visual cortex 113 days post-injection of a PVALB subclass specific AAV vector. Scale bar: 1 mm. Higher magnification image of the boxed region showing (B) anti-PVALB and (C) overlay of anti-GFP and anti-PVALB signal. Scale bars: 250  $\mu$ m. D, Epifluorescence photomicrograph of native SYFP2 fluorescence in a fixed brain slice from macaque primary motor cortex at 64 days post-injection of a layer 5 extratelencephalic subclass specific AAV vector. Scale bar: 500  $\mu$ m.

### 2. Behavioral and neurophysiological manipulation

To demonstrate the utility of this injection technique for neurophysiological and behavioral optogenetic manipulations, we performed three experiments, each on a different monkey (*Macaca mulatta*). In the first experiment (Fig. 4A-D), we injected AAV vectors carrying the channelrhodopsin-2 transgene (AAV1-hSyn1-ChR2-mCherry) into the left superior colliculus (SC). We injected every 250  $\mu$ m at multiple depths of the left SC for a total of 12  $\mu$ L. In the second experiment (Fig. 4E-G), we injected 3  $\mu$ L of AAV1-hSyn-ArchT-EYFP solution into the nucleus reticularis tegmenti pontis (NRTP). In the third experiment (Fig. 4H-K), we injected 24  $\mu$ L of AAV9-L7-ChR2-mCherry solution into the cerebellum<sup>6</sup>. Six to eight weeks after each injection, we inserted into the brain an optical fiber and a tungsten recording electrode via a double-barrel guide tube (Fig. 1G).

Fig. 4B shows the response of an SC neuron to blue light (450 nm). Continuous light (1.2 sec) at 40 mW produced a series of consecutive action potentials (Fig. 4B, top). Light pulses of 1 ms duration failed to evoke action potentials at 40 mW (Fig. 4B, middle), but did evoke action potentials reliably at 160 mW, the only other power level tested, with a latency of  $2.7 \pm 0.6$  ms (Fig. 4B, bottom). A pulse train (160 mW, frequency: 300 Hz, duty cycle: 15%, duration: 300ms) evoked saccades consistently with an average latency of  $97 \pm 32$  ms, a mean amplitude of  $10.4^\circ$  and mean angle of  $47^\circ$  (upward and to the right; Fig. 4C).

Consistent with studies that modified saccade gain using subthreshold electrical stimulation of the SC<sup>11,12</sup>, optical stimulation of the SC after 15, 18 and 20° left- and downward (225°) saccades gradually reduced saccade gain (Fig. 4D). This gain decrease required ~250 trials (green circles) to return to the pre-adaptation gain (black circles), confirming its basis in long-term plasticity.

In the second experiment (Fig. 4E), we optogenetically suppressed the mossy fiber projection from the nucleus reticularis tegmenti pontis (NRTP) to the oculomotor vermis (OMV) of the cerebellar cortex (lobules VIc and VII). Fig. 4F

shows fluorescently labeled mossy fibers and their rosettes (inset) in the OMV. We delivered yellow laser light (589 nm) to the OMV via optical fiber and used a nearby tungsten electrode to record Purkinje cell activity. Fig. 4G shows simple spike activity before (gray) and after (orange) optogenetic inactivation of NRTP projections (Fig. 4G, top). Prior to the inactivation, the Purkinje cell exhibited a double burst pattern for 12° rightward saccades (Fig. 4G, middle, gray). During optogenetic inactivation, the firing rate decreased and changed to a burst-pause pattern (Fig. 4G, middle, orange). Comparing these two response patterns suggests that the inhibited mossy fiber input to Purkinje cells influences the saccade deceleration phase by driving the second burst (Fig. 4G, middle, green). The variability of rightward saccades was reduced during optogenetic inactivation, consistent with the idea that some of the trial-to-trial variability in saccade metrics is due to variability in the signals carried by mossy fibers (Fig. 4G, bottom, orange).

In the third experiment (Fig. 4H), we optogenetically stimulated Purkinje cells of the OMV (Fig. 4I). A train of short light pulses (1.5 ms pulse, 65 mW, 50 Hz) increased the simple spike activity of an isolated Purkinje cell (Fig. 4J, top). A single 1.5 ms light pulse frequently evoked >1 simple spike action potential (Fig. 4J, bottom). Optogenetic simple spike activation, timed to occur during a saccade (10 ms long light pulse, 60 mW), increased saccade amplitude (Fig. 4K), confirming the disinhibitory role of Purkinje cells on the oculomotor burst generator.

Fig. 4 Summary of three optogenetic experiments performed in awake monkeys. A–D, Experiment 1, pan-neuronal excitation: viral injection, laser stimulation, and unit recording were conducted in the superior colliculus (A). B, Representative unit activity evoked by laser stimulation. C, Horizontal (top) and vertical (middle) components of eye movements and raster plot of unit activity (bottom) evoked by laser stimulation. D, A representative session of saccade adaptation induced by laser stimulation. Stimulation (100 0.5-ms laser pulses) was delivered 80 ms after each saccade (inset). Saccade gain (saccade amplitude / target amplitude) decreased gradually across trials. E–G, Experiment 2, pathway specific inhibition: a viral vector was injected into the nucleus reticularis tegmenti pontis, and laser stimulation (60 mW, continuous) and unit recording were conducted in the oculomotor vermis (E). F, Histological section of the oculomotor vermis showing labelled mossy fibers (scale bar: 1mm) and their rosettes (inset, scale bar: 100  $\mu$ m). G, Purkinje cell activity (top: raster, middle: average firing rate) and trajectories of visually guided saccades (bottom) with and without laser stimulation. Grey: laser off trials, orange: laser on trials, green: difference between grey and orange. H–K, Experiment 3, cell type-specific activation: viral injection, laser stimulation, and unit recording were conducted in the oculomotor vermis (H). I, Histological section of the oculomotor vermis showing labelled Purkinje cells. Scale bar: 100  $\mu$ m. J, Simple spike activity of a Purkinje cell evoked by laser stimulation. Top: raster plot from 14 trials. Bottom: voltage trace from a single representative trial. K, trajectories of visually guided saccades with and without laser stimulation. A 10-ms light pulse during saccades increased their amplitudes. Individual saccade trajectories (cyan) and their average (blue) on laser-on trials. Individual saccade trajectories (light grey) and their average (dark grey) on laser-off trials. The light was 450 nm for Experiments 1 and 3 and was 589 nm for Experiment 2.

## DISCUSSION: (3–6 paragraphs)

Advances in NHP optogenetics have created a need for accurate, reliable intracranial injection methods. Critical steps in this protocol include constructing high-quality cannulas, loading them without introducing bubbles, and selecting injection sites that are not too close together. We find that injections  $\geq 1$  cm apart usually transduce non-overlapping regions of the cerebral cortex, but this heuristic is dependent on viral serotype, titer, promoter, volume, target, and method of detection. Selecting injection sites that are not directly connected avoids potential confounds produced by opsin trafficking along axons and the propensity that some AAV serotypes have for retrograde transduction.

Advantages of the method described in this report are that it is inexpensive, uses sterilizable and disposable components, and has the ability to target diverse brain areas of any depth. It also permits control of injection speed and volume by virtue of the speed with which the air valve can be controlled. Air pressure can be increased transiently to

dislodge a clog and then reduced quickly to avoid subsequent over-injection that would be produced by sustained pressure as is produced by some mechanical pumps. Disposable components reduce the risk of cross-contamination between injection sites.

The method we describe can be used to inject NHPs while anesthetized and in a stereotaxic frame (Fig. 3) or alert and head-fixed (Fig. 4). The former has the advantage of allowing injections to be targeted in stereotaxic coordinates, and it allows visual confirmation of cannula penetration through an acute durotomy (incising the dura in an awake monkey, through a chronic craniotomy, has a high risk of infection). The latter approach has the advantages of reducing the number of survival surgeries and therefore the stress to the animal, being compatible with electrophysiological recordings during behavior, and using the same coordinate frame and instrumentation used to insert optical fibers for post-injection experiments. Our injection technique in awake monkeys could be further improved by making injections through artificial dura<sup>13-15</sup>. This would confer the additional advantages of direct visualization of injection sites and the subsequent tissue fluorescence that indicates successful transduction.

### Alternative techniques

Several other AAV injection techniques have been used in NHPs. Recently, a multi-channel injection device was developed to deliver AAV vectors uniformly to large NHP cortical regions<sup>16</sup>. Similar results can be obtained using convection-enhanced delivery<sup>17,18</sup>. These methods aim to maximize transduction spread—an important goal, but one that is distinct from the spatial precision our method aims to achieve.

An alternative method that we have used in the past is to inject AAV vectors through a length of borosilicate tubing that is beveled to a sharp tip on one end and attached to a Hamilton syringe on the other<sup>5,6</sup>. This method has much in common with the method described in this paper: the viral vector is held in a length of tubing, the space in the tubing behind the virus is filled with dyed oil, and flow of the virus is monitored via the movement of the oil-virus meniscus. This alternative technique requires less equipment and preparation, but it requires drawing oil into the borosilicate tubing through the beveled tip by negative pressure and loading the vector via the same route subsequently. This inevitably results in traces of oil delivered to the brain. Additionally, in our experience, the borosilicate tubing must have a diameter of ~350  $\mu\text{m}$  to penetrate dura even when beveled and therefore causes greater mechanical damage than the thinner metal cannula described in this report (Fig. 2D). We use 30G because its critical buckling load is high enough to mediate dura penetration despite a 1-10 cm length, because it fits the Teflon tubing tightly, and because it rarely clogs. We have used 33G tubing for injection when tissue damage was particularly concerning but found that it clogs and bends more easily and is more difficult to mate with the PTFE tubing. 36G is not stiff enough to penetrate dura mater.

A second alternative injection technique is to mate the output of the picopump to a back of a vector-loaded, pulled-glass pipette<sup>19</sup>. The vector is forced from the pipette tip by direct, intermittent pressure from the picopump, eliminating the need for oil. Similar to the single-tube method explained above, the lack of any material junctions between the meniscus and the cannula tip reduces the risk of leaks. However, the sharp taper and delicate tips of glass pipettes prevent them from penetrating NHP dura or targeting deep structures.

**ACKNOWLEDGMENTS:** This study was supported by WaNPRC/ITHS P51OD010425 (JTT), National Institute of Health (NIH) grants EY023277 (R01 for YK), EY030441 (R01 for GH), MH114126 (RF1 to JTT, Boaz Levi, Ed Lein), EY028902 (R01 for RS), and made possible by NIH grants OD010425 (P51 for WaNPRC) and University of Washington Royalty Research Fund A148416. The authors would like to thank Yasmine El-Shamayleh and Victoria Omstead for histology, Refugio Martinez for viral vector cloning, Shane Gibson for AAV vector purification and titer determination, and John Mich for assistance with NHP brain tissue processing.

**DISCLOSURES:** The authors have nothing to disclose.

## REFERENCES:

- 1 Kojima, Y., Robinson, F. R. & Soetedjo, R. Cerebellar fastigial nucleus influence on ipsilateral abducens activity during saccades. *Journal of Neurophysiology*. **111** (8), 1553-1563, (2014).
- 2 Kojima, Y. & Soetedjo, R. Elimination of the error signal in the superior colliculus impairs saccade motor learning. *Proceedings of the National Academy of Sciences of the United States of America*. **115** (38), E8987-e8995, (2018).
- 3 Kojima, Y., Soetedjo, R. & Fuchs, A. F. Effects of GABA agonist and antagonist injections into the oculomotor vermis on horizontal saccades. *Brain Research*. **1366** 93-100, (2010).
- 4 Kojima, Y., Soetedjo, R. & Fuchs, A. F. Effect of inactivation and disinhibition of the oculomotor vermis on saccade adaptation. *Brain Research*. **1401** 30-39, (2011).
- 5 De, A., El-Shamayleh, Y. & Horwitz, G. D. Fast and reversible neural inactivation in macaque cortex by optogenetic stimulation of GABAergic neurons. *Elife*. **9**, (2020).
- 6 El-Shamayleh, Y., Kojima, Y., Soetedjo, R. & Horwitz, G. D. Selective Optogenetic Control of Purkinje Cells in Monkey Cerebellum. *Neuron*. 10.1016/j.neuron.2017.06.002, (2017).
- 7 Mich, J. K. *et al.* Functional enhancer elements drive subclass-selective expression from mouse to primate neocortex. *Cell Rep*. **34** (13), 108754, (2021).
- 8 Graybuck, L. T. *et al.* Enhancer viruses and a transgenic platform for combinatorial cell subclass-specific labeling. *bioRxiv*. 10.1101/525014 525014, (2020).
- 9 Michel, J., Benninger, D., Dietz, V. & van Hedel, H. J. Obstacle stepping in patients with Parkinson's disease. Complexity does influence performance. *Journal of Neurology*. **256** (3), 457-463, (2009).
- 10 Chan, K. Y. *et al.* Engineered AAVs for efficient noninvasive gene delivery to the central and peripheral nervous systems. *Nature Neuroscience*. **20** (8), 1172-1179, (2017).
- 11 Kaku, Y., Yoshida, K. & Iwamoto, Y. Learning signals from the superior colliculus for adaptation of saccadic eye movements in the monkey. *Journal of Neuroscience*. **29** (16), 5266-5275, (2009).
- 12 Soetedjo, R., Fuchs, A. F. & Kojima, Y. Subthreshold activation of the superior colliculus drives saccade motor learning. *Journal of Neuroscience*. **29** (48), 15213-15222, (2009).
- 13 Kleinbart, J. E. *et al.* A Modular Implant System for Multimodal Recording and Manipulation of the Primate Brain. *Annu Int Conf IEEE Eng Med Biol Soc*. **2018** 3362-3365, (2018).
- 14 Arieli, A., Grinvald, A. & Slovin, H. Dural substitute for long-term imaging of cortical activity in behaving monkeys and its clinical implications. *Journal of Neuroscience Methods*. **114** (2), 119-133, (2002).
- 15 Ruiz, O. *et al.* Optogenetics through windows on the brain in the nonhuman primate. *Journal of Neurophysiology*. **110** (6), 1455-1467, (2013).
- 16 Fredericks, J. M. *et al.* Methods for mechanical delivery of viral vectors into rhesus monkey brain. *Journal of Neuroscience Methods*. **339** 108730, (2020).
- 17 Bankiewicz, K. S. *et al.* Convection-enhanced delivery of AAV vector in parkinsonian monkeys; in vivo detection of gene expression and restoration of dopaminergic function using pro-drug approach. *Experimental Neurology*. **164** (1), 2-14, (2000).
- 18 Yazdan-Shahmorad, A. *et al.* Widespread optogenetic expression in macaque cortex obtained with MR-guided, convection enhanced delivery (CED) of AAV vector to the thalamus. *Journal of Neuroscience Methods*. **293** 347-358, (2018).
- 19 Nathanson, J. L., Yanagawa, Y., Obata, K. & Callaway, E. M. Preferential labeling of inhibitory and excitatory cortical neurons by endogenous tropism of adeno-associated virus and lentivirus vectors. *Neuroscience*. **161** (2), 441-450, (2009).